International Journal of Solid Materials
Vol. 1, Issue 1, 2019, Pages 51-77
Published Online on March 30, 2019

http://jyotiacademicpress.org

STRESS ANALYSIS OF MULTIPLE SHRINK-FITTED ELASTIC CYLINDERS UNDER THERMAL AND MECHANICAL LOADS

XIANG-FA WU, MOJTABA AHMADI and URACHING CHOWDHURY

Department of Mechanical Engineering
North Dakota State University
Fargo, North Dakota, 58108
USA
e-mail: xiangfa.wu@ndsu.edu

Abstract

Shrink-fitted parts are commonly structured in mechanical systems (e.g., bearing-shaft coupling). This paper is to perform the theoretical study of the stress and displacement fields in multiple shrink-fitted elastic cylinders (tubes) under thermal and mechanical loads. Based on classic elasticity, the problem is reduced to find the interface pressures of neighboring tubes via solving a system of tridiagonal linear algebraic equations with the interface pressures as unknowns. Formal solutions are derived for the entire stress and displacement fields in general multiple shrink-fitted elastic tubes, which can recover the classic solution in the reduced cases. Numerical scaling analysis is conducted to examine the effects of interference, temperature change and mechanical loads on the stress variation in the elastic tubes. A concise computer code is programmed to implement the theoretical formulation for efficient and reliable stress analysis of an arbitrary number of shrink-fitted elastic tubes subject to constant temperature change and/or inner and outer pressures. As examples, numerical results of the radial and circumferential stresses of two, three and five shrink-fitted elastic tubes of different materials are demonstrated and

Keywords and phrases: shrink fit, stress analysis, elastic cylinders, thermomechanical loads, elasticity.

Communicated by Kazem Reza Kashyzadeh.

Received March 9, 2019; Revised March 14, 2019

compared. The present study facilitates the theoretical stress and strength analysis of broad shrink-fitting problems for optimal design and manufacturing of various mechanical press and shrink fits.

1. Introduction

Press and shrink fits are commonly found in mechanical design and manufacturing to couple two or more typically cylindrical mechanical parts via interference fitting such as assembly of bearings and collars onto crankshafts, which offer a feasible mechanical strategy for design and low-cost assembly of compact, reliable shaft systems. Classic solutions to the interface pressure and entire stress and displacement fields in two shrink-fitted elastic cylinders/tubes of free thermal and mechanical loads are commonly utilized in mechanical designs [1], which were derived on the basis of the classic elasticity solution to an elastic tube subject to constant inner and out pressures [2]. Yet, many shrink-fitting problems faced in engineering practices are typically more complicated and often involve three-dimensional (3D) effect near the fitting edges [3], anisotropicity of the tube materials [4,5], plastic deformations [6], surface defects [7], coupling of torsion and shrink-fitted gear-shaft system [8], interlayer effect [9], fretting wear and fatigue of shrink-fitted railway axles [10], among others. In addition, mechanical loads coupled with temperature change are also very common in many mechanical systems such as the bearing-crankshaft assemblies in vehicle gearboxes and other mechanical shaft mechanisms subject to seasonal temperature change in environment, while no general exact solutions are available in the literature for the stress and displacement fields of such shrink-fit problems though a few recent approaches have been made in the special cases with some extent of simplifications [11, 12]. Therefore, further study on this classic topic is still desired in order to facilitate the design and strength analysis of multiple shrink-fitted elastic tubes subject to general loads of temperature change and inner and outer pressures.

This study is aimed to formulate a general theoretical framework and elasticity solutions to multiple shrink-fitted elastic tubes subject to temperature change and inner/outer pressures. Classic elasticity solution to the stress and displacement fields of an elastic tube subject to inner and outer pressures is first summarized as it is the theoretical basis of the present work. Then, the general solutions to the interface contact pressure and the stress and displacement fields of two arbitrary shrink-fitted elastic tubes are derived, which will be further used for developing the general formal solution to the interface contact pressures of multiple shrink-fitted elastic tubes. The resulting system of tridiagonal linear algebraic equations with the interface contact pressures as the unknowns can be solved conveniently in a numerical manner. A few cases of two, three, and five shrink-fitted elastic tubes will be considered to demonstrate the efficiency and universality of the present method.

2. Problem Formulation and Solution

Consider a general case of n shrink-fitted elastic tubes, in which the number of each tube is labelled as $i = 1, 2, \ldots, n$ from the most inner tube to the most outside tube as shown in Figure 1. All the tubes are assumed to be homogeneous, isotropically elastic, and the Young's modulus, Poisson's ratio, and coefficient of thermal expansion of the i-th tube are designated as E_i, ν_i, and $\alpha_i (i = 1, 2, \ldots, n)$, respectively. The i-th interface is denoted as the interface between the (i–1)-th and i-th tubes, and the corresponding interference at the i-th interface is assumed as $\delta_i (i = 1, 2, \ldots, n-1)$ at reference temperature T_0 of the multiple elastic tubes. Hereafter, $r_{i-1} (i = 1, 2, \ldots, n)$ stands for the radius of the inner surface of the i-th tube; the radius of the outer surface of the i-th tube is $r_i + \delta_i (i = 1, 2, \ldots, n-1)$. The radius of the outer surface of the n-th tube is denoted as r_n. In the limiting cases, $r_0 = 0$ corresponds to the inner tube to be solid (i.e., the 1st-tube is a solid cylinder), and $r_n \to \infty$

corresponds to the outer n-th tube to be an infinite elastic body. The pressure on the i-th interface is denoted as $p_i (i = 1, 2, \ldots, n-1)$, and p_0 and p_n indicate the external pressures loaded on the inner surface of the 1st-tube and the outer surface of the n-th tube, respectively. Besides the mechanical loads (pressures) p_0 and p_n, the elastic tubes are assumed subject to a constant temperature change ΔT with respect to the reference temperature T_0. Under the above geometries, material properties as well as thermal and mechanical loads, the solution to the nontrivial stress and displacement fields of each elastic tube is important to the design and failure analysis of a shrink-fitted cylinder/tube system.

Hereafter, a brief overview is first made on the classic solution to the stress and displacement fields of an elastic tube subject to inner and outer pressures, which is treated in the planar stress state. Then, a general formal solution to two arbitrary shrink-fitted tubes is derived, which is further utilized for formulating a set of governing equations of general multiple shrink-fitted elastic tubes.

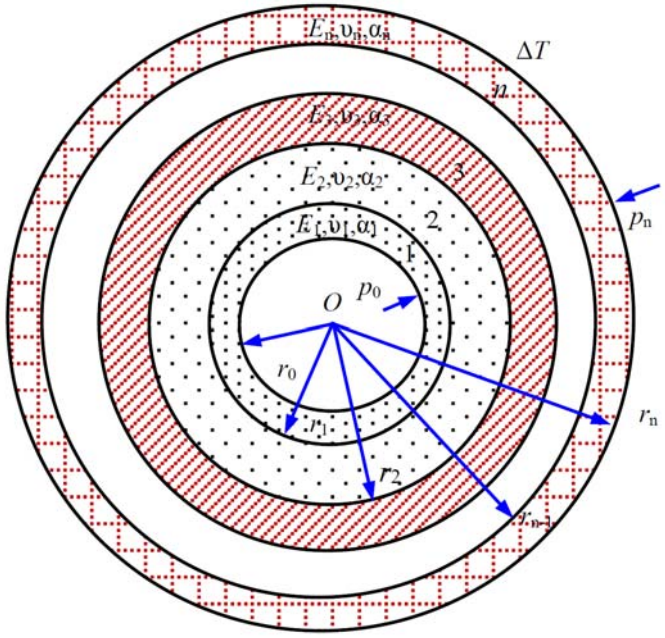

Figure 1. Schematic diagram of multiple shrink-fitted elastic tubes subject to constant temperature change ΔT and inner and outer pressures p_0 and p_n.

2.1. Stress and displacement fields of an elastic tube subject to inner and outer pressures

Consider a circular tube of homogeneous, isotropically elastic material (with the Young's modulus E and Poisson's ratio ν) as illustrated in Figure 2, in which a and b denote the inner and outer radii of the tube, respectively; p_i and p_o stand for the pressures loaded on the inner surface $r = a$ and the outer surface $r = b$, respectively. The nontrivial stress and displacement fields (σ_{rr}, $\sigma_{\theta\theta}$, and u_r) of such a classic axisymmetric elasticity problem are available in the literature as [2]

$$\sigma_{rr} = \frac{a^2 b^2}{b^2 - a^2} \frac{p_o - p_i}{r^2} + \frac{p_i a^2 - p_o b^2}{b^2 - a^2}, \tag{1}$$

$$\sigma_{\theta\theta} = -\frac{a^2b^2}{b^2 - a^2}\frac{p_o - p_i}{r^2} + \frac{p_i a^2 - p_o b^2}{b^2 - a^2}, \tag{2}$$

$$u_r = \frac{1-\upsilon}{E}\frac{(p_i a^2 - p_o b^2)r}{b^2 - a^2} - \frac{1+\upsilon}{E}\frac{(p_o - p_i)a^2 b^2}{(b^2 - a^2)r}. \tag{3}$$

In the limiting case of $a \to 0$, solutions (1)-(3) reduce to the stress and displacement fields of a solid cylinder subject to constant pressure p_o on the surface such that $\sigma_{rr} = \sigma_{\theta\theta} = -p_o$ and $u_r = -(1-\nu)p_o r / E$. Besides, in the limiting case of $b \to \infty$, solutions (1)-(3) reduce to the stress and displacement fields of a circular hole cut into an infinite elastic body under constant inner pressure p_i and remote compressive traction p_o as

$$\sigma_{rr} = (p_o - p_i)\frac{a^2}{r^2} - p_o, \tag{4}$$

$$\sigma_{\theta\theta} = -(p_o - p_i)\frac{a^2}{r^2} - p_o, \tag{5}$$

$$u_r = -\frac{1-\upsilon}{E}p_o r - \frac{1+\upsilon}{E}(p_o - p_i)\frac{a^2}{r}. \tag{6}$$

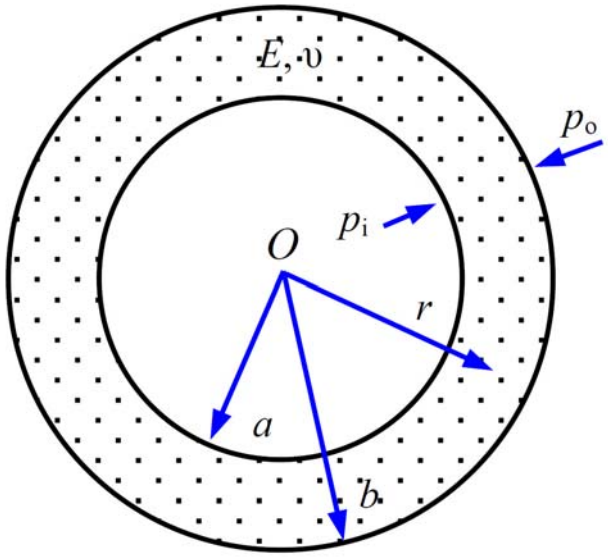

Figure 2. A circular elastic tube subject to inner and outer pressures.

2.2. Interface pressure and stress/displacement fields of multiple shrink-fitted elastic tubes subject to constant temperature change and inner and outer pressures

Now let us consider two representative neighboring tubes [i.e., the i-th and $(i+1)$-th tubes] out of a system of multiple shrink-fitted elastic tubes as illustrated in Figure 1. The notations of these two representative tubes are indicated in Figure 3, in which p_{i-1}, p_i, and p_{i+1} stand for the pressures in the inner surface [i.e., $(i-1)$-th interface], i-th interface, and outer surface [i.e., $(i+1)$-th interface], respectively. When a constant temperature change ΔT is applied to all the tubes, the inner radii of the i-th and $(i+1)$-th tubes become $r_{i-1}(1+\alpha_i \Delta T)$ and $r_i(1+\alpha_{i+1}\Delta T)$; correspondingly, the outer radii of the two tubes are $(r_i+\delta_i)(1+\alpha_i \Delta T)$ and $(r_{i+1}+\delta_{i+1})(1+\alpha_{i+1}\Delta T)$. Thus, the interference at the i-th interface after constant temperature change ΔT, i.e., thermal interference, is

$$\Delta_i = (r_i + \delta_i)(1 + \alpha_i \Delta T) - r_i(1 + \alpha_{i+1}\Delta T)$$

$$= r_i(\alpha_i - \alpha_{i+1})\Delta T + \delta_i(1 + \alpha_i \Delta T), \tag{7}$$

where $i = 1, 2, \ldots, n-1$ corresponding to each of the $(n-1)$ interfaces of the shrink-fitting problem with n elastic tubes. When $\Delta T = 0$, $\Delta_i = \delta_i$. For a general shrink-fitting problem, the thermal interference Δ_i at each interface results in a deformation compatibility condition. In the present case, $\Delta_i (i = 1, 2, \ldots, n-1)$ is equivalent to the difference of radial deformations of the inner and outer tubes at i-th interface $(i = 1, 2, \ldots, n-1)$ subject to inner and outer pressures at the current temperature $T + \Delta T$, i.e., the i-th tube is loaded with p_{i-1} and p_i while the $(i+1)$-th tube is loaded with p_i and p_{i+1} at their inner and outer surfaces, respectively, as shown in Figure 3. Therefore, the corresponding deformation compatibility condition at the i-th $(i = 1, 2, \ldots, n-1)$ interface can be expressed as

$$\Delta_i = u_r^{(i+1)}\big|_{r=r_i(1+\alpha_{i+1}\Delta T)} - u_r^{(i)}\big|_{r=(r_i+\delta_i)(1+\alpha_i \Delta T)}, \tag{8}$$

where

$$u_r^{(i+1)}\big|_{r=r_i(1+\alpha_{i+1}\Delta T)} = \frac{1}{E_{i+1}} \frac{r_i(1+\alpha_{i+1}\Delta T)}{(r_{i+1}+\delta_{i+1})^2 - r_i^2} \{(1-\upsilon_{i+1})[p_i r_i^2 - p_{i+1}(r_{i+1}+\delta_{i+1})^2]$$

$$- (1+\upsilon_{i+1})(p_{i+1} - p_i)(r_{i+1}+\delta_{i+1})^2\}, \tag{9}$$

is the radial displacement of the inner surface of the $(i+1)$-th tube, and

$$u_r^{(i)}\big|_{r=(r_i+\delta_i)(1+\alpha_i\Delta T)} = \frac{1}{E_i} \frac{(r_i+\delta_i)(1+\alpha_i\Delta T)}{(r_i+\delta_i)^2 - r_{i-1}^2} \{(1-\upsilon_i)[p_{i-1} r_{i-1}^2 - p_i(r_i+\delta_i)^2]$$

$$- (1+\upsilon_i)(p_i - p_{i-1}) r_{i-1}^2\}, \tag{10}$$

is the radial displacement of the outer surface of the i-th tube.

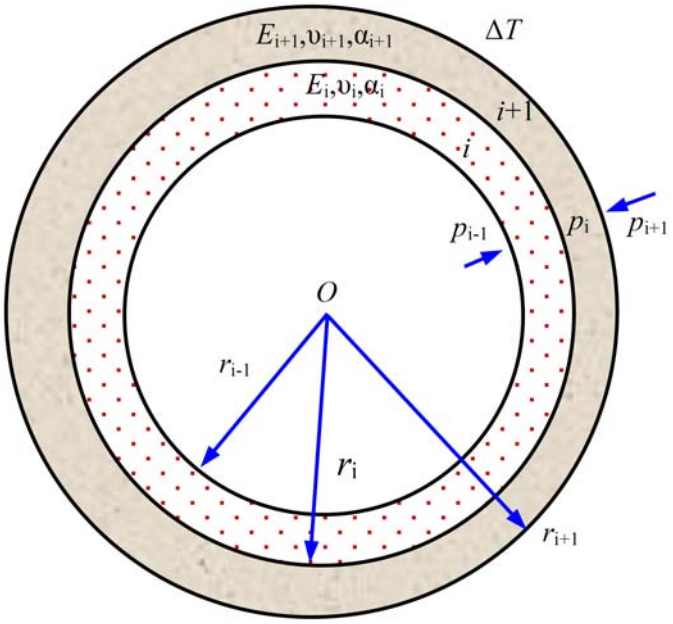

Figure 3. Two representative neighboring tubes in multiple shrink-fitted elastic tubes subject to constant temperature change ΔT and inner and outer pressures p_{i-1} and p_{i+1}.

Substitution of (9) and (10) into (8) leads to a representative algebraic equation relating the interfacial pressures p_{i-1}, p_i, and p_{i+1} to the thermal interference Δ_i as

$$a_{i,i-1}p_{i-1} + a_{i,i}p_i + a_{i,i+1}p_{i+1} = \Delta_i, \tag{11}$$

where $a_{i,i-1}$, $a_{i,i}$, and $a_{i+1,i}$ are coefficients as

$$a_{i,i-1} = -\frac{2}{E_i}\frac{(r_i + \delta_i)(1 + \alpha_i \Delta T)}{[(r_i + \delta_i)/r_{i-1}]^2 - 1}, \tag{12}$$

$$a_{i,i} = \frac{1}{E_i}\frac{(r_i + \delta_i)(1 + \alpha_i \Delta T)}{[(r_i + \delta_i)/r_{i-1}]^2 - 1}\{(1 - \upsilon_i)[(r_i + \delta_i)/r_{i-1}]^2 + (1 + \upsilon_i)\}$$

$$+ \frac{1}{E_{i+1}}\frac{r_i(1 + \alpha_{i+1}\Delta T)}{[(r_{i+1} + \delta_{i+1})/r_i]^2 - 1}\{(1 - \upsilon_{i+1})$$

$$+ (1 + \upsilon_{i+1})[(r_{i+1} + \delta_{i+1})/r_i]^2\}, \tag{13}$$

$$a_{i,i+1} = -\frac{2}{E_{i+1}}\frac{r_i(1 + \alpha_{i+1}\Delta T)}{1 - [r_i/(r_{i+1} + \delta_{i+1})]^2}, \tag{14}$$

and $i = 1, 2, \ldots, n-1$ represents the i-th interface of n shrink-fitted elastic tubes. As a result, relation (11) leads to a system of tridiagonal algebraic equations of the order $(n-1)$ for n shrink-fitted elastic tubes as

$$\begin{cases} a_{1,0}p_0 + a_{1,1}p_1 + a_{1,2}p_2 = \Delta_1, \\ a_{2,1}p_1 + a_{2,2}p_2 + a_{2,3}p_3 = \Delta_2, \\ \cdots \\ a_{n-2,n-3}p_{n-3} + a_{n-2,n-2}p_{n-2} + a_{n-2,n-1}p_{n-1} = \Delta_{n-2}, \\ a_{n-1,n-2}p_{n-2} + a_{n-1,n-1}p_{n-1} + a_{n-1,n}p_n = \Delta_{n-1}, \end{cases} \tag{15}$$

which can be expressed in a well-formatted, concise matrix form:

$$\begin{bmatrix} a_{1,1} & a_{1,2} & 0 & 0 & 0 & \cdots & 0 \\ a_{2,1} & a_{2,2} & a_{2,3} & 0 & 0 & \cdots & 0 \\ 0 & a_{3,2} & a_{3,3} & a_{3,4} & 0 & \cdots & 0 \\ 0 & 0 & a_{4,3} & a_{4,4} & a_{4,5} & \cdots & 0 \\ \cdots & \cdots & \cdots & \cdots & \cdots & \cdots & \cdots \\ 0 & 0 & \cdots & 0 & a_{n-2,n-3} & a_{n-2,n-2} & a_{n-2,n-1} \\ 0 & 0 & \cdots & 0 & 0 & a_{n-1,n-2} & a_{n-1,n-1} \end{bmatrix}$$

$$\begin{Bmatrix} p_1 \\ p_2 \\ p_3 \\ \cdot \\ \cdot \\ p_{n-2} \\ p_{n-1} \end{Bmatrix} = \begin{Bmatrix} \Delta_1 - a_{1,0}p_0 \\ \Delta_2 \\ \Delta_3 \\ \Delta_4 \\ \cdots \\ \Delta_{n-2} \\ \Delta_{n-1} - a_{n-1,n}p_n \end{Bmatrix}. \quad (16)$$

Solving Equation (16) results in pressure $p_i (i = 1, 2, \ldots, n-1)$ at $(n-1)$ interfaces of n shrink-fitted elastic tubes, which can be further used for determining the stress and displacement fields in each elastic tube via triggering the elasticity solutions (1)-(3) of an elastic tube subject to inner and outer pressures. Within the framework of elasticity, the present solutions to the interface pressures of multiple shrink-fitted tubes are exact. In addition, it needs to be mentioned that a similar set of governing equations of the same system was obtained by Qiu and Zhou [11] in the case of some extent of approximations. In particular, temperature change induced radius variations in the elastic tubes were ignored.

3. Case Studies and Scaling Analysis of Shrink-Fitted Elastic Tubes

3.1. Stress and displacement fields of two shrink-fitted elastic tubes subject to constant temperature change and inner and outer pressures

This is the special case of two elastic tubes in shrink-fitting as studied in Subsection 2.2. Rewriting Equation (11) with $\delta_2 = 0$ (as r_2 is the outer radius of the outer tube based on the present symbol convention) leads to

$$a_{1,0}p_0 + a_{1,1}p_1 + a_{1,2}p_2 = \Delta_1, \tag{17}$$

where coefficients $a_{1,0}$, $a_{1,1}$, $a_{1,2}$ and Δ_1 are determined as

$$a_{1,0} = -\frac{2}{E_1}\frac{(r_1 + \delta_1)(1 + \alpha_1\Delta T)}{[(r_1 + \delta_1)/r_0]^2 - 1}, \tag{18}$$

$$a_{1,1} = \frac{1}{E_1}\frac{(r_1 + \delta_1)(1 + \alpha_1\Delta T)}{[(r_1 + \delta_1)/r_0]^2 - 1}\{(1 - \upsilon_1)[(r_1 + \delta_1)/r_0]^2 + (1 + \upsilon_1)\}$$

$$+ \frac{1}{E_2}\frac{r_1(1 + \alpha_2\Delta T)}{(r_2/r_1)^2 - 1}[(1 - \upsilon_2) + (1 + \upsilon_2)(r_2/r_1)^2], \tag{19}$$

$$a_{1,2} = -\frac{2}{E_2}\frac{r_1(1 + \alpha_2\Delta T)}{1 - (r_1/r_2)^2}, \tag{20}$$

$$\Delta_1 = (r_1 + \delta_1)(1 + \alpha_1\Delta T) - r_1(1 + \alpha_2\Delta T)$$

$$= r_1(\alpha_1 - \alpha_2)\Delta T + \delta_1(1 + \alpha_1\Delta T). \tag{21}$$

Thus, the interface pressure p_1 can be solved from (17) as

$$p_1 = (\Delta_1 - a_{1,0}p_0 - a_{1,2}p_2)/a_{1,1}, \tag{22}$$

where p_0 and p_2 are the external pressures acting on the inner and outer surfaces as given in the problem. Plugging p_0 and p_1 as well as p_1 and p_2 into (1)-(3), respectively, leads to the solutions to the nontrivial stress and displacement fields in the inner and outer elastic tubes. In the case of the two shrink-fitted tubes free of inner and outer pressures and subject to constant temperature change ΔT, Equation (22) leads to the interface pressure p_1 as

$$p_1 = \Delta_1 / a_{1,1} = -\frac{r_1(\alpha_1 - \alpha_2)\Delta T + \delta_1(1 + \alpha_1 \Delta T)}{\frac{1}{E_1}\frac{(r_1 + \delta_1)(1 + \alpha_1 \Delta T)}{[(r_1 + \delta_1)/r_0]^2 - 1}\{(1 - \upsilon_1)[(r_1 + \delta_1)/r_0]^2 + (1 + \upsilon_1)\}}$$

$$+ \frac{1}{E_2}\frac{r_1(1 + \alpha_2 \Delta T)}{(r_2 / r_1)^2 - 1}[(1 - \upsilon_2) + (1 + \upsilon_2)(r_2 / r_1)^2]. \qquad (23)$$

In the limiting case of constant temperature, i.e., $\Delta T = 0$, and further ignoring the small effect of the interference δ_1 on the radius r_1, Equation (23) is further simplified as

$$p_1 = -\frac{\delta_1}{r_1\left[\frac{1}{E_2}\left(\frac{r_2^2 + r_1^2}{r_2^2 - r_1^2} + \upsilon_2\right) + \frac{1}{E_1}\left(\frac{r_1^2 + r_0^2}{r_1^2 - r_0^2} - \upsilon_1\right)\right]}, \qquad (24)$$

which is the commonly used shrink-fit formula for predicting the interface pressure of two shrink-fitted cylinders in mechanical design [1]. The comparison of the accuracies of the interface pressure p_1 and the stress field (σ_{rr} and $\sigma_{\theta\theta}$) based on the present exact solution (23) and the commonly used formula (24) at varying temperature change ΔT and interference δ_1 will be made in Subsection 3.3.

3.2. Stress and displacement fields of three shrink-fitted elastic tubes subject to constant temperature change and inner and outer pressures

By following the same taken in Subsection 3.1, rewriting Equation (11) for $i = 1$ and 2 with $\delta_3 = 0$ leads to a set of simultaneous linear algebraic equations as

$$\begin{cases} a_{1,1}p_1 + a_{1,2}p_2 = \Delta_1 - a_{1,0}p_0, \\ a_{2,1}p_1 + a_{2,2}p_2 = \Delta_2 - a_{2,3}p_3, \end{cases} \tag{25}$$

where coefficients $a_{1,0}$, $a_{1,1}$, $a_{2,1}$ and Δ_1 are given according to (12)-(14) and (7) as

$$a_{1,0} = -\frac{2}{E_1}\frac{(r_1 + \delta_1)(1 + \alpha_1\Delta T)}{[(r_1 + \delta_1)/r_0]^2 - 1}, \tag{26}$$

$$a_{1,1} = \frac{1}{E_1}\frac{(r_1 + \delta_1)(1 + \alpha_1\Delta T)}{[(r_1 + \delta_1)/r_0]^2 - 1}\{(1 - \upsilon_1)[(r_1 + \delta_1)/r_0]^2 + (1 + \upsilon_1)\}$$

$$+ \frac{1}{E_2}\frac{r_1(1 + \alpha_2\Delta T)}{[(r_2 + \delta_2)/r_1]^2 - 1}\{(1 - \upsilon_2) + (1 + \upsilon_2)[(r_2 + \delta_2)/r_1]^2\}, \tag{27}$$

$$a_{1,2} = -\frac{2}{E_2}\frac{r_1(1 + \alpha_2\Delta T)}{1 - [r_1/(r_2 + \delta_2)]^2}, \tag{28}$$

$$a_{2,1} = -\frac{2}{E_i}\frac{(r_2 + \delta_2)(1 + \alpha_2\Delta T)}{[(r_2 + \delta_2)/r_1]^2 - 1}, \tag{29}$$

$$a_{2,2} = -\frac{1}{E_2}\frac{(r_2 + \delta_2)(1 + \alpha_2\Delta T)}{[(r_2 + \delta_2)/r_1]^2 - 1}\{(1 - \upsilon_2)[(r_2 + \delta_2)/r_1]^2 + (1 + \upsilon_2)\}$$

$$+ \frac{1}{E_3}\frac{r_2(1 + \alpha_3\Delta T)}{(r_3/r_2)^2 - 1}[(1 - \upsilon_3) + (1 + \upsilon_3)(r_3/r_i)^2], \tag{30}$$

$$a_{2,3} = -\frac{2}{E_3}\frac{r_2(1 + \alpha_3\Delta T)}{1 - (r_2/r_3)^2}, \tag{31}$$

$$\Delta_1 = (r_1 + \delta_1)(1 + \alpha_1 \Delta T) - r_1(1 + \alpha_2 \Delta T)$$

$$= r_1(\alpha_1 - \alpha_2)\Delta T + \delta_1(1 + \alpha_1 \Delta T), \tag{32}$$

$$\Delta_2 = (r_2 + \delta_2)(1 + \alpha_2 \Delta T) - r_2(1 + \alpha_3 \Delta T)$$

$$= r_2(\alpha_2 - \alpha_3)\Delta T + \delta_2(1 + \alpha_2 \Delta T). \tag{33}$$

The solution to (25) leads to the formal solution of interface pressures p_1 and p_2 as

$$p_1 = \frac{\begin{vmatrix} \Delta_1 - a_{1,0}p_0 & a_{1,2} \\ \Delta_2 - a_{2,3}p_3 & a_{2,2} \end{vmatrix}}{\begin{vmatrix} a_{1,1} & a_{1,2} \\ a_{2,1} & a_{2,2} \end{vmatrix}}, \tag{34}$$

$$p_2 = \frac{\begin{vmatrix} a_{1,1} & \Delta_1 - a_{1,0}p_0 \\ a_{2,1} & \Delta_2 - a_{2,3}p_3 \end{vmatrix}}{\begin{vmatrix} a_{1,1} & a_{1,2} \\ a_{2,1} & a_{2,2} \end{vmatrix}}. \tag{35}$$

With the interface pressures p_1 and p_2 solved in (34) and (35), the stress and displacement fields in the three shrink-fitted elastic tubes can be determined conveniently by using Equations (1)-(3). Yet, the detailed expansions of solutions (34) and (35) are inconvenient in practical use. In reality, it is more convenient to formulate the symbolic elements of the coefficient matrix and right column vector in Equation (16) based on (12)-(14) and (7) and then to solve Equation (16) numerically to obtain all the interface pressures p_i $(i = 1, 2, \ldots, n-1)$ of the multiple shrink-fitted elastic tubes. Consequently, with the interface pressures p_i $(i = 1, 2, \ldots, n-1)$, the stress and displacement fields in each elastic tube can be determined exactly by Equations (1)-(3) as to be demonstrated in Subsection 3.3.

3.3. Scaling analysis of dependencies of interface pressure and stresses upon temperature change and interferences in multiple shrink-fitted elastic tubes

3.3.1. Two shrink-fitted elastic tubes

Herein, comparative study is made to examine the effects of temperature change ΔT and interference δ on the interface pressure p_1 and stress fields (σ_{rr} and $\sigma_{r\theta}$) in two shrink-fitted elastic tubes based on the present exact solution (23) and the literature formula (24). Assume an aluminum-alloy tube and a steel tube to be shrink-fitted at reference temperature T_0 as shown in Figure 4. The material properties and geometries of the tubes are tabulated in Table 1, where δ is considered as a variable for the purpose of scaling analysis.

Based on (23) and (24), Figure 5 shows the variation of the interface pressure p_1 with respect to δ ranging from 0 to 1.6mm at four constant temperature changes of − 200°C, 0°C, 200°C, and 400°C, respectively, from T_0, in which the literature solution (24) is only used for the case of ΔT = 0°C. From Figure 5, it can be observed that as a general principle, the value of p_1 increases with increasing δ. At ΔT = 0°C, p_1 predicted by the present solution (23) is slightly higher than that predicted by (24); the difference between the values of p_1 predicted by (23) and (24) increases with increasing δ. Besides, the $p_1 - \delta$ relation is linear in (24) while it becomes nonlinear in the present solution (23). As a matter of fact, the literature solution (24) can be regarded as the linearization of the present solution (23) in the case of small δ compared to the tube radii.

In addition, given the value of δ, Figure 5 shows that the value of p_1 predicted by (23) increases nearly linearly with increasing ΔT in a large range from − 200°C to 400°C though p_1 given in (23) is nonlinear with respect to ΔT. The increasing tendency of p_1 with ΔT is due to the

configuration of two shrink-fitted tubes such that the inner tube (aluminum-alloy) has a higher coefficient of thermal expansion than that of the outer tube (steel). Thus, the inner tube has a larger radial expansion than the outer tube at temperature increase ΔT, i.e., a higher interface pressure. If the materials of the two tubes are reversed in the shrink-fitting assembly, p_1 will decrease with increasing ΔT.

Table 1. Material properties and geometries of shrink-fitted aluminum-alloy and steel tubes

Materials	Aluminum alloy (inner)	Carbon steel (outer)
Young's modulus	$E_{A1} = 71.7 \times 10^3$MPa	$E_{st} = 207 \times 10^3$MPa
Poisson's ratio	$\upsilon_{A1} = 0.333$	$\upsilon_{st} = 0.292$
Coefficient of thermal expansion	$\alpha_{A1} = 23.9 \times 10^{-6}/℃$	$\alpha_{st} = 10.8 \times 10^{-6}/℃$
Outer radius	$r_o = 40.0\text{mm} + \delta$	$R_o = 50.0$mm
Inner radius	$r_i = 30.0$mm	$R_i = 40.0$mm

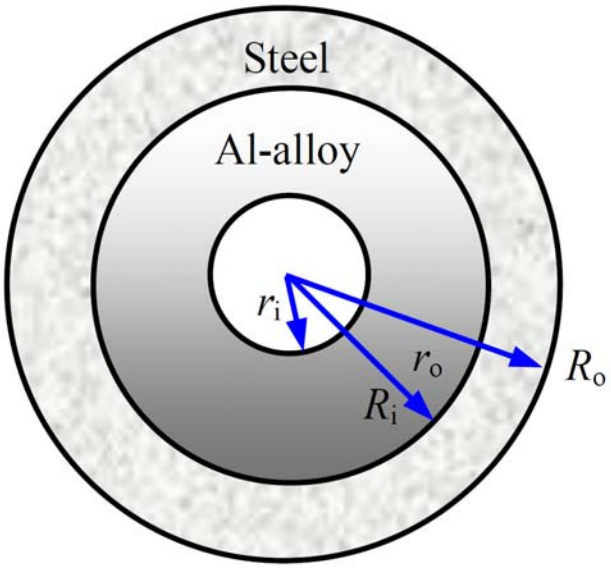

Figure 4. An aluminum-alloy tube shrink-fitted into a steel tube.

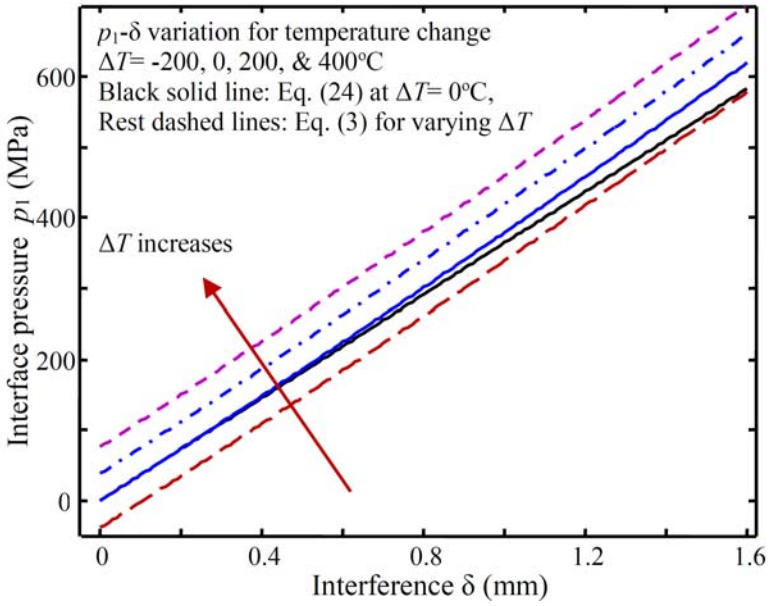

Figure 5. Variation of the interface pressure p_1 with respect to the interference δ of an aluminum-alloy tube shrink-fitted into a steel tube with pressure-free inner and outer surfaces and temperature change ΔT.

Figure 6 shows variations of the radial stress σ_{rr} and circumferential stress $\sigma_{\theta\theta}$ with respect to the tube radius r of an aluminum-alloy tube shrink-fitted into a steel tube with δ = 0.5mm and ΔT = 200°C. The inner and outer surfaces are assumed to be pressure-free. It is observed that the compressive σ_{rr} reaches its peak value at the interface, which is the interface pressure and reaches to zero at the inner and outer surfaces due to the pressure-free surface conditions. $\sigma_{\theta\theta}$ in the inner aluminum-alloy tube is compressive and its peak value occurs at the inner surface; in contrast, $\sigma_{\theta\theta}$ in the outer steel tube is tensile and its peak value occurs at the interface. In addition, the value of $\sigma_{\theta\theta}$ has a jump across the fitting interface due to the interference as well as the mismatch of the material properties across the interface. It needs to be mentioned that even in the case of two elastic tubes of identical material

in shrink-fitting, the jump of $\sigma_{\theta\theta}$ across the interface still exists due to the discontinuity of the circumferential strain across the interface that is induced by δ.

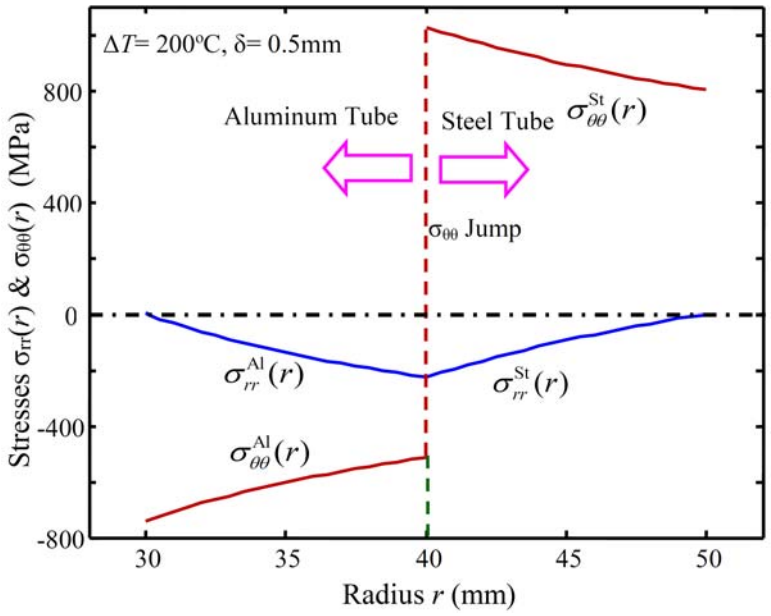

Figure 6. Variations of the radial stress σ_{rr} and circumferential stress $\sigma_{\theta\theta}$ with respect to the radius r of an aluminum-alloy tube shrink-fitted into a steel tube with interference δ = 0.5mm and temperature change ΔT = 200°C (with pressure-free inner and outer surfaces).

3.3.2. General numerical scheme for stress analysis of multiple shrink-fitted elastic tubes

Based on the theoretical formulation in Subsection 2.2, efficient computer code can be programmed for fast and reliable analysis of the stress and displacement fields in multiple shrink-fitted elastic tubes subject to constant temperature change ΔT as well as inner and outer pressures p_0 and p_n. For the numerical process, a concise Matlab® code is programmed to demonstrate the numerical procedure according to Equations (11)-(16) in the follows.

To evidence the effectiveness of this numerical approach, Figures 7(a) and 7(b) show two examples of the numerical solutions to the stress variations in three and five shrink-fitted elastic tubes subject to only ΔT = 200ºC and combination of ΔT = 200ºC, p_0 = 50MPa, and p_5 = 100MPa, respectively. Interferences at two interfaces of the three shrink-fitted elastic tubes are assumed to be identical as δ_i = 0.5mm (i = 1 and 2), while the interferences at the four interfaces of the five shrink-fitted tubes are also assumed to be identical as δ_i = 0.25mm. As shown in Figure 7, the material properties of the aluminum-alloy and steel tubes are given in Table 1, and the material properties of the copper tube are: Young's modulus: E_{Cu} = 119GPa, Poisson's ratio: ν_{Cu} = 0.326, and coefficient of thermal expansion: $\alpha_{Cu} = 17.1 \times 10^{-6}$. By following the symbol convention defined in Section 2, the nominal radii of the three shrink-fitted tube in Figure 7(a) are taken as r_1 = 30mm, r_2 = 40mm, r_3 = 50mm, and r_4 = 60mm (i.e., the inner radii of the tubes and the outer radius of the outer tube), and the nominal radii of the five shrink-fitted tubes in Figure 7(b) are taken r_1 = 30mm, r_2 = 40mm, r_3 = 50mm, r_4 = 60mm, r_5 = 70mm, and r_6 = 80mm.

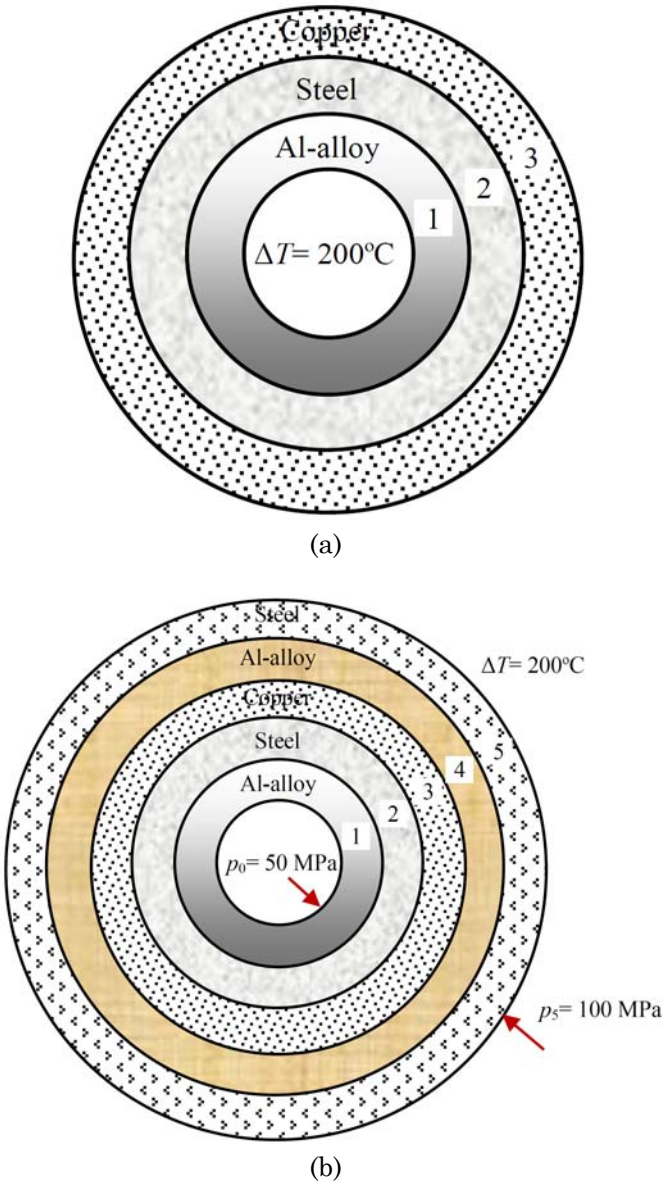

Figure 7. Configurations of three and five shrink-fitted elastic tubes. (a) Loaded with constant temperature change $\Delta T = 200^{o}C$ (interferences: $\delta_1 = \delta_2 = 0.5mm$); (b) Loaded with constant temperature change $\Delta T = 200^{o}C$, inner surface pressure $p_0 = 50MPa$ and outer surface pressure $p_5 = 100MPa$ (interferences: $\delta_1 = \delta_2 = \delta_3 = \delta_4 = 0.25mm$).

Figure 8 shows the variations of σ_{rr} and $\sigma_{\theta\theta}$ with respect to r of the three shrink-fitted elastic tubes subject to constant temperature change ΔT = 200°C. It can be found that σ_{rr} is compressive and continuously varying in the tubes while reaching zero at the inner and outer surfaces due to the pressure-free surface conditions, and the value of σ_{rr} reaches its peak value at the aluminum/steel interface. $\sigma_{\theta\theta}$ is compressive in the inner aluminum-alloy tube while tensile in the steel and copper tubes; $\sigma_{\theta\theta}$ jumps across the two interfaces as also observed in the case of two shrink-fitted elastic tubes. The value of $\sigma_{\theta\theta}$ reaches its peak value at the two interfaces and the outer surface.

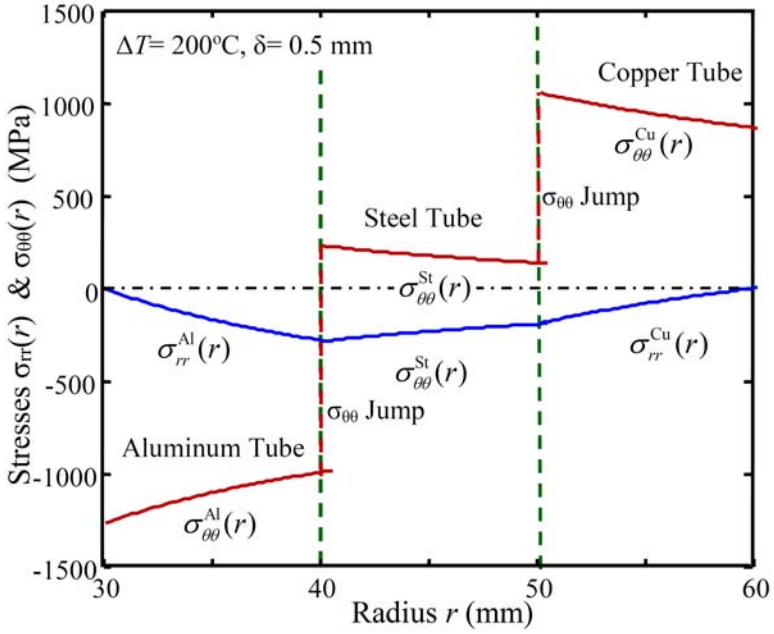

Figure 8. Variations of the radial stress σ_{rr} and circumferential stress $\sigma_{\theta\theta}$ with respect to the radius r of three shrink-fitted elastic tubes of aluminum-alloy, steel and copper at interference δ = 0.5mm and temperature change ΔT = 200°C (pressure-free inner and outer surfaces).

Furthermore, Figure 9 shows the variations of σ_{rr} and $\sigma_{\theta\theta}$ with respect to the radius r of five shrink-fitted elastic tubes subject to constant temperature change ΔT = 200°C and inner and outer surface pressures p_0 = 50MPa and p_5 = 100MPa. It can be found that σ_{rr} is compressive and continuously varying in the tubes while reaching − 50MPa at the inner surface and − 100MPa at the outer surface as designated by the problem, and the value of σ_{rr} reaches its peak value at the inner aluminum/steel interface. In addition, $\sigma_{\theta\theta}$ is compressive in the four inner tubes while tensile in the most outer steel tubes due to specific tube assembly, interferences, temperature change, and pressures on the inner and outer surfaces; $\sigma_{\theta\theta}$ jumps across the four interfaces as also observed in two and three shrink-fitting elastic tubes aforementioned. The peak value of $\sigma_{\theta\theta}$ appears at the interfaces and the outer surface in this particular shrink-fitting problem.

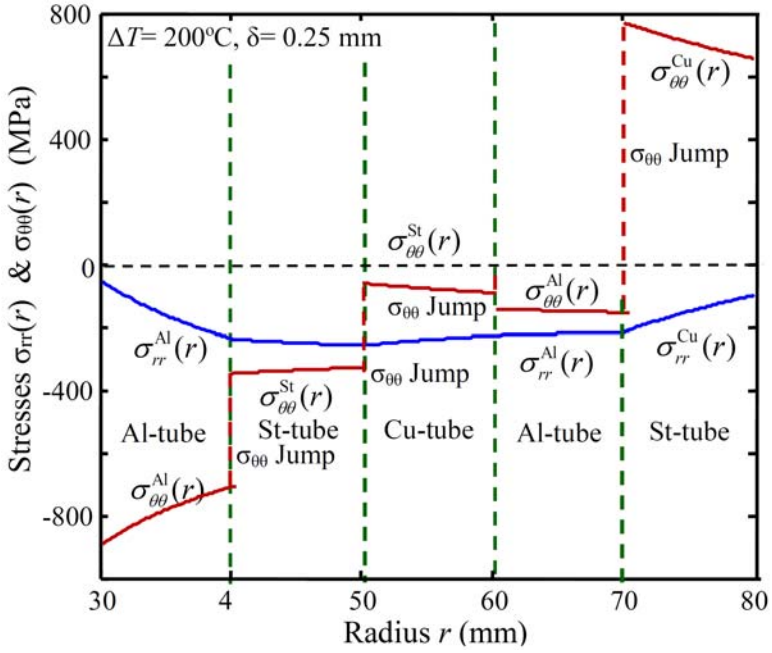

Figure 9. Variations of the radial stress σ_{rr} and circumferential stress $\sigma_{\theta\theta}$ with respect to the radius r of five shrink-fitted elastic tubes of aluminum-alloy, steel, copper, aluminum-alloy and steel at interference $\delta = 0.25\text{mm}$ and constant temperature change $\Delta T = 200^{\circ}\text{C}$, inner surface pressure $p_0 = 50\text{MPa}$ and outer surface pressure $p_5 = 100\text{MPa}$.

From the above scaling analysis of two, three and five shrink-fitting elastic tubes, the following conclusions can be drawn. σ_{rr} is compressive in multiple shrink-fitted elastic tubes with constant temperature change and pressure-free or compressive inner and outer surfaces; its peak value appears at one of the interfaces. $\sigma_{\theta\theta}$ is compressive in the most inner tube while $\sigma_{\theta\theta}$ in the outside tubes may be compressive or tensile depending on the tube assembly, interference $\delta_i (i = 1, 2, \ldots, n-1)$, temperature change ΔT, and pressures p_0 and p_n on the inner and outer surfaces, respectively; its peak value appears at one of the

interfaces or the outer surface. Therefore, for multiple shrink-fitted elastic tubes with identical interference, the peak stress level may appear at the first inner interface or the outer surface, and it is highly possible that material cracking or yielding happens at the first inner interface or the outer surface.

It needs to be emphasized that the present study is based on purely linear elasticity analysis of multiple shrink-fitted elastic tubes with several simplifications as aforementioned. For instance, the surface roughness, material nonlinearity, and plasticity of the tubes are not considered yet. Furthermore, in a typical shrink-fitting assembly in reality, the stress and deformation analysis will be 3D as the common configuration of such an assembly is usually in the form of a short tube (ring) shrink-fitted onto a long elastic cylinder, or coaxial cylinders. Nevertheless, the present theoretical formulation and related numerical scheme based on assumption of axisymmetric deformation provide the quick, reliable understanding of the stress variations in such idealized shrink-fitting tube systems, which is valuable in their design and strength estimate.

4. Concluding Remarks

Shrink-fitting cylindrical (tubular) systems are commonly utilized in various mechanical mechanisms. For the purpose of fast, reliable stress and deformation analysis of such systems, a theoretical framework and related numerical approach have been successfully formulated. It has been shown herein that the stress analysis of such multiple shrink-fitted elastic tubes can be reduced to solving a governing system of tridiagonal linear algebraic equations with the interface pressures as the unknowns. Once these interface pressures are extracted from solving the resulting set of linear algebraic equations, the stress analysis of the elastic tubes can be further determined one tube by one tube with the assistance of the classic elasticity solution of an elastic tube. To demonstrate the efficiency

and effectiveness of the present method, a concise computer code has been programmed and used for high-efficiency, accurate stress analysis of two, three and five shrink-fitted elastic tubes of different materials subject to constant temperature changes and inner and outer pressures. The present theoretical formulation and numerical scheme extend the stress and strength analysis of broad shrink-fitting problems consisting of an arbitrary number of elastic tubes of varying elastic materials, interferences, and inner and outer pressures.

Acknowledgement

Partial support of this research by the National Science Foundation, NASA EPSCoR (NASA Grant # NNX07AK91A, seed grant: 43500-2490-FAR018640), and Department of Mechanical Engineering NDSU at NDSU is gratefully appreciated.

References

[1] R. G. Budynas and J. K. Nisbett, Shigley's Mechanical Engineering Design, (10th Edition), McGraw Hill, New York, USA, 2015.

[2] S. P. Timoshenko and J. N. Goodier, Theory of Elasticity, (2nd Edition), McGraw-Hill, New York, USA, 1951.

[3] P. Pedersen, On shrink fit analysis and design, Computational Mechanics 37(2) (2006), 121-130.

DOI: https://doi.org/10.1007/s00466-005-0664-7

[4] I. Tsukrov and B. Drach, Elastic deformation of composite cylinders with cylindrically orthotropic layers, International Journal of Solids and Structures 47(1) (2010), 25-33.

DOI: https://doi.org/10.1016/j.ijsolstr.2009.09.005

[5] D. Croccolo and M. de Agostinis, Analytical solution of stress and strain distributions in press fitted orthotropic cylinders, International Journal of Mechanical Science 71 (2013), 21-29.

DOI: https://doi.org/10.1016/j.ijmecsci.2013.03.002

[6] A. N. Erashan and T. Akis, Yield of two-layer shrink-fitted composite tubes subject to radial pressure, Forsch Ingenieurwes 69(4) (2005), 187-196.

DOI: https://doi.org/10.1007/s10010-005-0001-5

[7] H. Boutoutaou, M. Bouaziz and J. F. Fontaine, Modeling of interference fits taking form defects of the surfaces in contact into account, Materials and Design 32(7) (2011), 3692-3701.

DOI: https://doi.org/10.1016/j.matdes.2011.03.059

[8] S. J. Chu, T. K. Jeong and E. H. Jung, Effect of radial interference on torque capacity of press-and shrink-fit gears, International Journal of Automotive Technology 17(5) (2016), 763-768.

DOI: https://doi.org/10.1007/s12239-016-0075-0

[9] M. Zhao, Z. Wu and H. Cai, Stress analysis of compound cylinders with interlayer pressure after autofrettages, International Journal of Pressure Vessels and Piping 163 (2018), 63-67.

DOI: https://doi.org/10.1016/j.ijpvp.2018.03.002

[10] D. Zeng, Y. Zhang, L. Lu, L. Zou and S. Zhu, Fretting wear and fatigue in press-fitted railway axle: A simulation study of the influence of stress relief groove, International Journal of Fatigue 118 (2019), 225-236.

DOI: https://doi.org/10.1016/j.ijfatigue.2018.09.008

[11] J. Qiu and M. Zhou, Analytical solution for interference fit for multi-layer thick-walled cylinders and the application in crankshaft bearing design, Applied Sciences 6(6) (2018), Article 167.

DOI: https://doi.org/10.3390/app6060167

[12] U. A. Campos and D. E. Hall, Simplified Lamé's equations to determine contact pressure and hoop stress in thin-walled press-fits, Thin-Walled Structures 138 (2019), 199-207.

DOI: https://doi.org/10.1016/j.tws.2019.02.008

■